Evaluation of terrestrial carbon cycle models with atmospheric CO_2 measurements: Results from transient simulations considering increasing CO_2, climate, and land-use effects

R. J. Dargaville,[1,2] M. Heimann,[3] A. D. McGuire,[4] I. C. Prentice,[3] D. W. Kicklighter,[5] F. Joos,[6] J. S. Clein,[1] G. Esser,[7] J. Foley,[8] J. Kaplan,[3] R. A. Meier,[1] J. M. Melillo,[5] B. Moore III,[9] N. Ramankutty,[8] T. Reichenau,[7] A. Schloss,[9] S. Sitch,[10] H. Tian,[5] L. J. Williams,[11] and U. Wittenberg[7]

Received 1 April 2001; revised 20 August 2002; accepted 21 August 2002; published 19 November 2002.

[1] An atmospheric transport model and observations of atmospheric CO_2 are used to evaluate the performance of four Terrestrial Carbon Models (TCMs) in simulating the seasonal dynamics and interannual variability of atmospheric CO_2 between 1980 and 1991. The TCMs were forced with time varying atmospheric CO_2 concentrations, climate, and land use to simulate the net exchange of carbon between the terrestrial biosphere and the atmosphere. The monthly surface CO_2 fluxes from the TCMs were used to drive the Model of Atmospheric Transport and Chemistry and the simulated seasonal cycles and concentration anomalies are compared with observations from several stations in the CMDL network. The TCMs underestimate the amplitude of the seasonal cycle and tend to simulate too early an uptake of CO_2 during the spring by approximately one to two months. The model fluxes show an increase in amplitude as a result of land-use change, but that pattern is not so evident in the simulated atmospheric amplitudes, and the different models suggest different causes for the amplitude increase (i.e., CO_2 fertilization, climate variability or land use change). The comparison of the modeled concentration anomalies with the observed anomalies indicates that either the TCMs underestimate interannual variability in the exchange of CO_2 between the terrestrial biosphere and the atmosphere, or that either the variability in the ocean fluxes or the atmospheric transport may be key factors in the atmospheric interannual variability. *INDEX TERMS:* 0315 Atmospheric Composition and Structure: Biosphere/atmosphere interactions; *KEYWORDS:* carbon dioxide, atmospheric transport modeling, terrestrial biosphere modeling, model evaluation, seasonal cycle, interannual variability

Citation: Dargaville, R. J., et al., Evaluation of terrestrial carbon cycle models with atmospheric CO_2 measurements: Results from transient simulations considering increasing CO_2, climate, and land-use effects, *Global Biogeochem. Cycles*, *16*(4), 1092, doi:10.1029/2001GB001426, 2002.

1. Introduction

[2] There is considerable uncertainty in the net exchange of carbon between the terrestrial biosphere and the atmosphere. The IPCC budget estimates uptake due to CO_2 fertilization, nitrogen fertilization, climate effects and forest regrowth of 1.9 ± 1.3 Gt C a^{-1} for the period 1980–1989 [*Bolin et al.*, 2000]. We need to improve our understanding of how the processes which govern the uptake and release of carbon from the large terrestrial reservoir have responded to past natural and anthropogenic perturbations so that we

[1]Institute of Arctic Biology, University of Alaska, Fairbanks, Alaska, USA.
[2]Now at Laboratoire des Sciences du Climate et de l'Environnement, Gif-sur-Yvette, France.
[3]Max-Plank-Institut für Biogeochemie, Jena, Germany.
[4]U.S. Geological Survey, Alaska Cooperative Fish and Wildlife Research Unit, University of Alaska, Fairbanks, Alaska, USA.
[5]Ecosystem Center, Marine Biological Laboratory, Woods Hole, Massachusetts, USA.
[6]Physics Institute, University of Bern, Bern, Switzerland.
[7]Institut für Pflanzenökologie, Justus-Liebeg-Universität, Giessen, Germany.
[8]Center for Sustainability and the Global Environment, University of Wisconsin, Madison, Wisconsin, USA.
[9]Complex Systems Research Center, Institute for the Study of Earth, Oceans and Space, University of New Hampshire, Durham, New Hampshire, USA.
[10]Potsdam Institute for Climate Impact Research, Potsdam, Germany.
[11]Electric Power Research Institute, Palo Alto, California, USA.

0886-6236/02/2001GB001426$12.00

can reduce the budget uncertainty and gain a better understanding of how the complex feedbacks between climate change and the carbon budget will behave in the future. Various approaches for estimating the regional scale fluxes are available, such as process-based Terrestrial Carbon Models (TCMs) [*Melillo et al.*, 1995; *Cramer et al.*, 1999; *Heimann et al.*, 1998; *McGuire et al.*, 2000, 2001], bookkeeping analyses [*Houghton*, 1999] and atmospheric inversions [*Ciais et al.*, 1995; *Fan et al.*, 1998; *Rayner et al.*, 1999; *Bousquet et al.*, 1999, 2000; *Battle et al.*, 2000]. Of these approaches, process-based TCMs are the best option for improving our understanding of the processes contributing to the variability in the terrestrial carbon budget, and therefore their development and evaluation are important research pursuits.

[3] The importance of the TCM approach in global carbon cycle research has led to the development of a number of models [*Cramer et al.*, 1999; *Melillo et al.*, 1995; *McGuire et al.*, 2001; *Heimann et al.*, 1998; *Schimel et al.*, 2000]. The TCMs all have different approaches to modeling the exchange of carbon between the atmosphere and biosphere, different sensitivities to the climate data. They were each developed with different research goals (e.g., understanding the role of the nitrogen cycle, or the impact of dynamic vegetation) and thus produce a range of results. It is therefore important to evaluate the performance of the TCMs to help improve the representation of terrestrial processes that influence the exchange of carbon between the biosphere and the atmosphere, and to ensure that the correct model is used for the correct purpose.

[4] One reason for large range of estimates of net biosphere carbon exchange is that TCMs often use point measurements of carbon fluxes which need to be extrapolated in time and space so that they can be used to develop and evaluate the models. The method we use here for evaluating the TCMs is to use the network of atmospheric CO_2 monitoring stations, which are very effective in integrating the response of carbon fluxes over large regions.

[5] To evaluate the TCMs with atmospheric CO_2 data, a model of the atmospheric transport is required to simulate the transport of the signal from the surface fluxes to the monitoring stations. Previous studies using this method have found that the TCMs in general reproduce the main features of the atmospheric seasonal cycle observations [*Heimann et al.*, 1998; *Nemry et al.*, 1999; *McGuire et al.*, 2000]. These studies used TCMs that were run to equilibrium and therefore could not consider the interannual variability or trends in the observed and simulated atmospheric concentrations. An important difference between this study and previous similar studies is that we used TCMs that were run in transient mode, with forcing data including increasing CO_2, climate change and land-use change. Therefore we can evaluate the trends and interannual variability in the carbon fluxes by comparing them with the atmospheric CO_2 measurements.

[6] The amplitude of the seasonal cycle of atmospheric CO_2 has been observed to be increasing at several atmospheric monitoring stations [*Keeling et al.*, 1996; *Randerson et al.*, 1997]. The reason for this increase is not well understood but is thought to be due to increased atmospheric temperatures leading to a longer high-latitude growing season [*Chapin et al.*, 1996; *Keeling et al.*, 1996; *Randerson et al.*, 1999] and/or the effect of increased atmospheric CO_2 on carbon exchange [*Kohlmaier et al.*, 1989]. Also, increased disturbance (i.e., fire), which may also be related to global warming [*Zimov et al.*, 1999] may play a role as disturbance acts to reduce the stand age and therefore affects the carbon dynamics. Using the same TCM runs as this study, *McGuire et al.* [2001] examined the seasonal cycle amplitude changes simulated at Mauna Loa using a simple atmospheric box model approach. The analysis indicated that the CO_2 fertilization effect simulated by all models contributed to the increasing trend in amplitude at Mauna Loa, while the contributions of climate and land-use change varied among the models.

[7] In this paper we will expand upon the work of *McGuire et al.* [2001] by using the modeled fluxes as surface sources for a 3-dimensional atmospheric transport model and examine the simulated and observed concentrations at 15 monitoring stations. We compare the shape and phase of the average seasonal cycle, the trends in amplitude of the seasonal cycle, and the interannual variability in concentration anomalies produced by the models with the observations.

2. Model and Data Description

2.1. Terrestrial Carbon Models

[8] The main processes represented in the TCMs are net primary production (NPP) and heterotrophic respiration (R_H). The NPP flux is the difference between the uptake of carbon by vegetation through photosynthesis and the loss of carbon through autotrophic respiration by the vegetation, while R_H represents the release of CO_2 to the atmosphere through decomposition of organic matter. These fluxes are calculated using algorithms which employ temperature, precipitation, radiation, soil and plant functional type information, amongst others.

[9] The four TCMs in this study are the High Resolution Biosphere Model (HRBM [*Esser et al.*, 1994]), the Integrated Biosphere Simulator (IBIS [*Foley et al.*, 1996]), the Lund-Potsdam-Jena Dynamic Vegetation model (LPJ [*Sitch*, 2000]), and the Terrestrial Ecosystem Model (TEM [*Tian et al.*, 1999]. The long-term carbon budgets from these models are described in more detail by *McGuire et al.* [2001]. As well as the transient nature of the simulations, these simulations are also different from previous studies because they include information about land-use change. Whereas previous studies using TCMs had assumed a natural vegetation coverage, *McGuire et al.* [2001] consider the direct impacts of land clearing for crops, the CO_2 effects of cropland production and harvest, and the effects of cropland abandonment on terrestrial carbon dynamics. The models were run with three scenarios: increasing CO_2 alone (S1), increasing CO_2 and climate variability (S2), and increasing CO_2, climate variability and land-use change (S3).

[10] The net carbon exchange (NCE) in the TCMs is described by

$$NCE = R_H - NPP + E_F + E_C + E_P \quad (1)$$

where E_F is the loss of terrestrial carbon due to fires (only in LPJ and IBIS), E_C is the carbon flux during the conversion of natural ecosystems to cultivation, and E_P is the sum of carbon emissions from the decomposition of products generated from the clearing of land for agriculture (paper and wood) and of products harvested from cropland. The NPP and R_H fluxes are reported monthly, while E_F, E_C and E_P are reported annually. Therefore, in these simulations only NPP and R_H will directly influence the seasonal cycle. The land-use change fluxes will have an indirect effect because of effects on carbon pools, but without the seasonality in E_F, E_C and E_P it is not possible to determine their direct contribution to the atmospheric seasonal cycle, although we could expect that the E_C and E_P fluxes (which have relatively small values compared to the R_H and NPP fluxes) would have only a small direct impact on the seasonal cycle. The impact of E_F has a significant impact on the seasonal cycle at tropical and southern high latitude stations [*Iacobellis et al.*, 1994; *Wittenberg et al.*, 1998] it does not appear to substantially influence the seasonal cycle of northern stations [*Wittenberg et al.*, 1998].

[11] The TCMs were driven by three data sets that contained interannual and longer-term variability. For the time period we are examining in this study, the atmospheric CO_2 data were obtained from *Keeling et al.* [1995]. Temperature and precipitation were derived from work by *Jones* [1994] and *Hulme* [1992]. The historical land-use data set was derived from work by *Ramankutty and Foley* [1998, 1999]. These data are described in more detail by *McGuire et al.* [2001].

[12] Each of the four models uses different approaches to modeling carbon exchange based on the input data. HRBM uses statistical relationships of temperature and precipitation to calculate NPP, which is modified according to CO_2 concentrations and soil characteristics. The other models calculate gross primary production and autotrophic respiration and output NPP as the difference between the two. TEM models the effects of nitrogen dynamics on carbon dynamics. LPJ has a climate sensitive fire regime, while IBIS has constant fire regime. Both LPJ and IBIS are Dynamic Global Vegetation Models, and represent how carbon dynamics are influenced by interactions among plant functional types, and how these interactions influence the recruitment, growth, and mortality of plant functional types. Each model tracks different numbers of carbon pools, and each model has different algorithms to describe the processes of photosynthesis, respiration and water balance. These differences are discussed in more detail by *McGuire et al.* [2001].

2.2. Fossil and Ocean Fluxes

[13] The ocean and fossil sources also contribute to the atmospheric seasonal cycle. We have estimated the contributions of these components by running source estimates for fossil [*Andres et al.*, 1996] and ocean [*Doney et al.*, 2002] through our transport model. The fossil source we use does not have a seasonal cycle; however, the seasonality in atmospheric transport produces seasonal variations at the observing sites. The actual seasonality of the fossil sources is not well known as the economic figures used to calculate the sources are only available annually.

[14] Neither the ocean or fossil flux estimates used here have interannual variability. For the fossil case this is reasonable as the fossil emission inventories [*Marland et al.*, 2002] show smooth changes from year to year. However the fossil source has certainly increased over the time period of this study, which we have not taken into account in this study. The oceans fluxes are somewhat less well understood with some lines of evidence suggesting small interannual variability in the ocean fluxes compared with the terrestrial biosphere [*Bousquet et al.*, 2000; *Lee et al.*, 1998; *Feely et al.*, 1999], but comparable variability has been shown by others [*Rayner et al.*, 1999; *Joos et al.*, 1999; *LeQuéré et al.*, 2000]. This has important consequences for the modeled concentration anomalies which will be discussed later.

2.3. Atmospheric Transport Model

[15] Our implementation of MATCH (Model of Atmospheric Transport and Chemistry version 2.0 [*Rasch et al.*, 1997; *Mahowald et al.*, 1997]) is a semi-Lagrangian transport model that runs with 24 levels in the vertical on hybrid sigma-pressure coordinates. The horizontal resolution is 2.8° by 5.6° (latitude by longitude). The model was run with a time step of 1.5 hours in an 'offline' mode with archived data from a control run of the Middle Atmosphere Community Climate Model II (MACCM2 [*Waugh*, 1997]). The subgrid scale processes of convection and diffusion were parameterized using the *Hack* [1994] and *Holtslag and Boville* [1993] schemes. Because only 1 year of winds was used, interannual variability in the atmospheric CO_2 concentrations due to the transport is ignored. The effect of interannual in transport on the atmospheric seasonal cycle has not yet been studied in detail, however preliminary results suggest that the impact is not insignificant [*Dargaville et al.*, 2000], and may be a source of discrepancy between the observations and model results.

[16] *Law et al.* [1996] made intercomparisons of a number of widely used transport models (TransCom project). Although MATCH was not a participant in TransCom1, the online version of the model (CCM2/NCAR [*Erickson et al.*, 1996]) did participate. The CCM2/NCAR model produced an interhemispheric difference (IHD) of 3.1 ppmv for the fossil source case. We have run the TransCom fossil source case for our version of MATCH and get a similar IHD of 2.9 ppmv. The results show that MATCH has comparable large-scale transport to the other transport models widely used such as GISS (IHD = 2.8 ppmv) and TM2 (IHD = 3.4). *Law et al.* [1996] also ran a biosphere source case with seasonal variability which showed that the transport models generally fell into one of two groups; those that produce a seasonal "rectifier" (positive north-south gradient due to a deeper mixed layer during the growing season in which NPP dominates [*Denning et al.*, 1995] and those that do not. The CCM2/NCAR does simulate a rectifier (IHD = 0.8), as does MATCH (IHD = 0.8) in runs we have performed. In comparison TM2 (IHD = −0.1) and GISS (IHD = 0.2) do not simulate a significant rectifier effect. *Law et al.* [1996] concluded that it was the models with explicit planetary boundary layers formulations (such

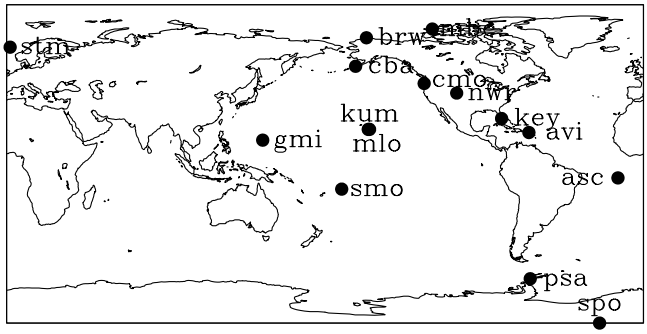

Figure 1. Location of 15 NOAA/CMDL CO_2 monitoring sites. Note that Mauna Loa and Kumukahi share almost the same latitude and longitude, but that Kumukahi is at sea level while Mauna Loa is at 3400 m. See Figure 3 for abbreviation expansions.

as MATCH) that produce a rectifier. This is a contentious issue as the true strength of the rectifier is not known.

2.4. Atmospheric CO_2 Data Set

[17] In each of the atmospheric transport runs, we subsampled the modeled CO_2 concentrations for comparison with observations at 15 NOAA Climate Monitoring and Diagnostic Laboratory (CMDL) stations. We choose only stations with at least 70% complete records over the period 1980–1992, and this resulted in the sites being mostly located in the Northern Hemisphere, and are mostly in and around North America and the Pacific (Figure 1). The modeled CO_2 concentrations were compared with the GLOBALVIEW (GV) data set [*GLOBALVIEW-CO2*, 1999]. These data have approximately weekly resolution with 48 equally spaced time points for each year. In the GV data set, missing values have been filled. The replacements for the missing data were calculated based on the observed signal from years without data gaps and from surrounding stations [*Masarie and Tans*, 1995]. We choose to use estimates for the missing data rather than have gaps as the gaps could alter the appearance of the seasonal cycle, especially if data are missing at the time of maximum and minimum concentrations. The 70% criteria mentioned above is applied so that interpolation is kept to a minimum. Most of the sites are 90% or more complete. The sites are either coastal or on islands (except South Pole and Niwot Ridge), as the aim of the stations is to collect air uncontaminated by local source effects (''baseline'' selection). Therefore the air is sampled when the wind is coming from over the ocean and not the land. The advantage is that the air sampled is representative of large regions, while the drawback is that any signal from the terrestrial biosphere has to travel some distance from its source before being measured. This means that the signals from the different terrestrial regions become mixed and diluted, which makes identification of the region responsible for the observed signals a nontrivial task.

[18] Two of the stations we examine are at high altitudes that are not represented by the topography of our model. Both the NWR and MLO are stations that collect air samples at approximately 3400 m above sea level and are on steep peaks which are not resolved by the spatial resolution of the model. Therefore, to enable a comparison of the observations with the modeled concentrations, we took the modeled values from the model level which best matches the actual level of the stations. For MLO we used the sixth level above the surface (680 hPa), while for NWR we used the fifth (625 hPa).

3. Methods

[19] For each TCM the monthly net fluxes were aggregated from the TCM grid ($0.5^\circ \times 0.5^\circ$ resolution) to the coarser transport model grid ($2.8^\circ \times 5.6^\circ$). The atmospheric concentrations in the transport model were initialized with uniform values. The transport model was run with the TCM fluxes over the period July 1978 to December 1992, with the first six months of the run discarded so that the transport model had time to ''spin up.''

[20] The modeled concentrations were subsampled at every time step (1.5 hours) at each of the GV stations we examined. To make the modeled concentrations comparable with the observations we first calculated daily averages, then removed the long-term trend (the simulated concentrations decrease with time because the TCMs all calculate biosphere to be a long-term net sink of CO_2) by subtracting a smoothed spline [*Enting*, 1987]. We then fitted a spline with a much shorter smoothing period (one month) so that it fitted the concentrations very closely, and projected the spline onto the GV timescale. We removed the increasing trend from the GV observations by also subtracting a smoothed spline. This approach maintains the shape of the seasonal cycle. The first and last years of the runs and the observations (1979 and 1992) were used to detrend the data, but were not included in the average seasonal cycle or trend analysis to avoid problems associated with fitting the data at the ends of the time series. The simulated concentrations from the fossil and ocean flux runs were also detrended in the same fashion, and then the average seasonal cycle of each added to the detrended time series from each of the TCMs.

[21] From the detrended data an average annual cycle was calculated by averaging values at each point of the year across the 11-year period. The standard deviation of the observations was also calculated to indicate the interannual variability. To calculate the average amplitude and the phase timing of the seasonal cycle, each simulated year was analyzed and then the average for each feature was calculated (as opposed to finding the average seasonal cycle and taking the amplitude and phase from that, although the difference between the two approaches is small). The standard deviation of the amplitude and phases for the observations were also calculated. The amplitude was calculated by taking the difference between the maximum and minimum concentrations in each year. The amplitude trends were calculated by linear regression through the annual values. Uncertainties were estimated by taking the range of slopes within the 90% confidence limit of the regression. The phasing was determined by simply finding the time of maximum and minimum CO_2 concentration each year.

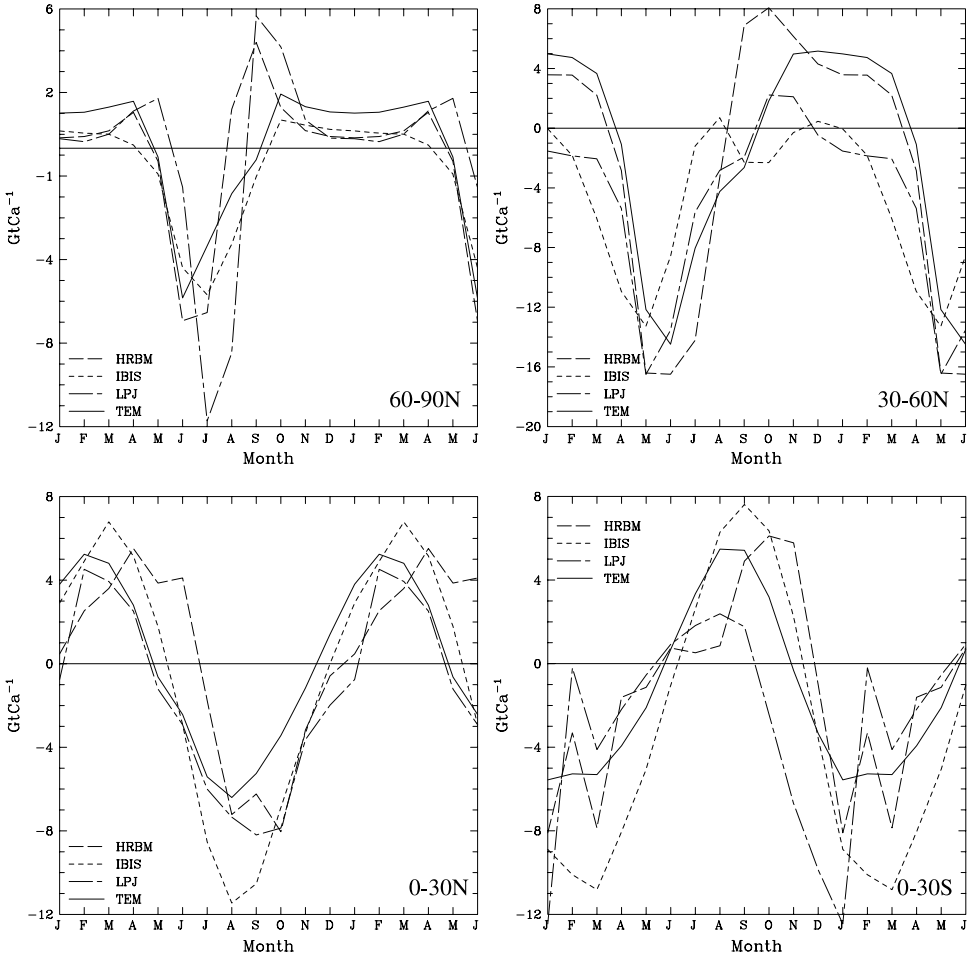

Figure 2. Average seasonal cycle aggregated over 30° latitude bands for the period 1980 to 1991 for the four biosphere models HRBM, IBIS, LPJ and TEM. The southern extratropical regions are not shown due to the small amount of biosphere is these regions. Note that the first 6 months of the annual cycle have been repeated.

[22] For the amplitude trend calculation we also used monthly NOAA/CMDL data without the data filling to test for possible biases introduced due to the filling. At each station the trends showed no statistical differences for the different data sets, but because of the data gaps in the monthly records there were larger uncertainties in the trend at some stations.

[23] Concentration anomalies were calculated by taking a 12-month running mean through the detrended time series of observed and simulated concentrations. To compare the observed and modeled anomalies we calculated linear regressions of the observed anomalies against the modeled anomalies. The slope and correlation values were recorded.

4. Results

[24] We present a brief analysis of the seasonal cycle of the TCM fluxes at a regional scale, and then examine the simulated atmospheric concentrations using the TCM fluxes as surface sources in MATCH. Only the S3 fluxes were used in the evaluation of the seasonal cycle and the concentration anomalies, while the evaluation of trends in the amplitude considers all three scenarios separately.

4.1. Terrestrial Carbon Model Fluxes

[25] The average seasonal cycles of the carbon fluxes for the period 1980–1991 for each model aggregated into 30° bands indicates that the models generally agree, with a drawdown of CO_2 during the spring and summer months, and a shorter growing period in the higher latitudes (Figure 2). In the tropics, the Northern Hemisphere is in the opposite phase to the Southern Hemisphere with the northern uptake occurring around August–September and the maximum southern uptake occurring around January–March. However, there are also some differences between the model estimates, with LPJ showing a larger and later summer drawdown compared with the other models in the 60°N–90°N band. Also in this region IBIS shows a release of CO_2 into the atmosphere late in summer and almost no release in the winter months. In the tropics there is a spread of results among the models, and no model stands out from the others. The goal in the remainder of this paper is to determine where these source patterns are

consistent with the atmospheric observations, and where there are discrepancies.

4.2. Average Seasonal Cycles at Observing Stations

[26] The comparison of the average seasonal cycles for each of the TCM transport runs with the observations indicates that the models generally simulate many of the characteristics of the seasonal cycle, including the spatial patterns of amplitude and phasing. (Figure 3). Note that the seasonal cycle from the ocean and fossil source simulations has been added to each TCM seasonal cycle. In the figures the first 6 months of the cycle have been repeated to make the cycle more apparent. The error bars shows the ±1 standard deviation for the observations. For stations north of the tropics (NWR, CMO, CBA, STM, BRW and MBC; see Figure 3 for abbreviation expansions), the observed atmospheric seasonal cycle has a maximum around April, a minimum about August following the spring and summer drawdown. At the Northern Hemisphere tropical stations (KEY, MLO, KUM and GMI) the amplitude is smaller, and tends to peak earlier and reach a minimum later, indicating a longer growing season than in higher northern latitudes (note the difference in vertical axes for the lower latitude sites). The Southern Hemisphere sites all exhibit small seasonal cycle amplitudes. In the Southern Hemisphere the contribution to the seasonal cycle by the oceans is significant, with between 0 and 13% of the amplitude coming from the ocean fluxes [*Randerson et al.*, 1997; *Heimann et al.*, 1998].

[27] Table 1 shows the root mean squares (RMS) for the difference between each TCM simulations and the observed seasonal cycles. The errors are smallest in the Southern Hemisphere and increase with latitude. TEM and HRBM consistently produce the smallest errors, with TEM doing the best in the northern extratropics.

4.2.1. Average Amplitude and Phase of the Seasonal Cycle of Atmospheric CO_2

[28] To distill information from the results in Figure 3 and to make interpretation easier, we have plotted the amplitude and phase timing for each of the seasonal cycles (Figure 4) and produced a table (Table 2) of qualitative measures of each model's performance. For both the observations and the transport runs over the period 1980 to 1991, the average amplitude of the seasonal cycle is smaller in the Southern Hemisphere than the Northern Hemisphere (Figure 4a). The amplitude increases with latitude in the Northern Hemisphere as the difference in summer and winter fluxes becomes more and more distinct. In the Northern Hemisphere the observations show a gradual increase in the seasonal amplitude from the equator to CBA and a flatter trend through the higher latitude sites. The simulations of all the models also demonstrate this pattern of amplitude with latitude, but tend to underestimate the magnitude of the amplitude by between 2 and 4 ppmv (Table 2). HRBM and TEM perform best overall, while the simulations with LPJ have amplitudes that are most similar in magnitude to the observations in the high latitudes, and the simulations with IBIS underestimate the amplitude by greatest degree. This is consistent with the source patterns in Figure 2, in which LPJ had the larger seasonal cycle. All the simulated amplitudes are less than the observations in the Northern Hemisphere tropics, with LPJ and IBIS underestimating by the most. An outlying result is the larger amplitude that LPJ produces at CMO; CMO is a coastal site, and the issue of data selection may be important. It is possible that the baseline selection criteria would reduce the simulated seasonal cycle, while in this experiment we have not considered the difficult task of simulating the selection criteria in subsampling the model.

4.2.2. Phasing of the Seasonal Cycle

[29] Figure 4b shows the timing of the minimum CO_2 concentration. The observations are characterized by a broad range in the timing of the minimum concentration for the southern tropical stations, mostly due to SMO, a smaller range for the southern high latitude stations, and a narrow range for the Northern Hemisphere stations (Figure 4b). The large tropical variability may be due to the phase of the seasonal cycle being sensitive to the timing of the wet and dry seasons, which vary with the ENSO phenomenon. In the Northern Hemisphere the timing has less variability as the amplitudes are larger and less sensitive to climate variability. In general, the timing of the minimum concentrations simulated by the TCMs agree well with the observations. An exception is the IBIS simulation at SPO, ASC and STM. The phase difference at SPO is probably due to the smaller amplitude IBIS exhibits in the Northern Hemisphere, which when transported to the southern high latitudes and combined with the ocean fluxes results in a reversal of phase compared with the observations. LPJ produces a minimum concentration too early at NWR, and the plot for NWR in Figure 3 shows that the simulated seasonal cycles for LPJ (and IBIS) fail to reproduce the general pattern in the observations. This might be due to transport error, however the TEM and HRBM simulations compare more favorably with the observations.

[30] The average timing of maximum concentration simulated by the models generally agrees with the timing of maximum concentrations in the observations (Figure 4c), although not as well as the minimum concentration timing. IBIS has phase discrepancies at SPO and PSA. There is a wide spread of model results at SMO and ASC for both the maximum and minimum timing, such that several of the simulations do not fall within the range of the observations. For these stations, the range of variability in the observations is almost as large as the annual amplitude (see Figure 3), possibly resulting from variability in the position of the ITCZ. At the Northern Hemisphere stations, the timing of the maximum concentrations simulated by the HRBM, IBIS and TEM are generally very close to the observations, but tend to be early in some cases. A notable result here is that LPJ has the maximum occurring too early at five of the Northern Hemisphere stations. From the source seasonal cycle in Figure 2 it can be seen that the LPJ source increase after the summer drawdown in the northern high latitudes is more exaggerated that the other TCMs, (although only a little more than HRBM) and is perhaps overshooting, resulting in the maximum concentrations occurring in autumn, rather than in spring as in the observations. At NWR, both LPJ and

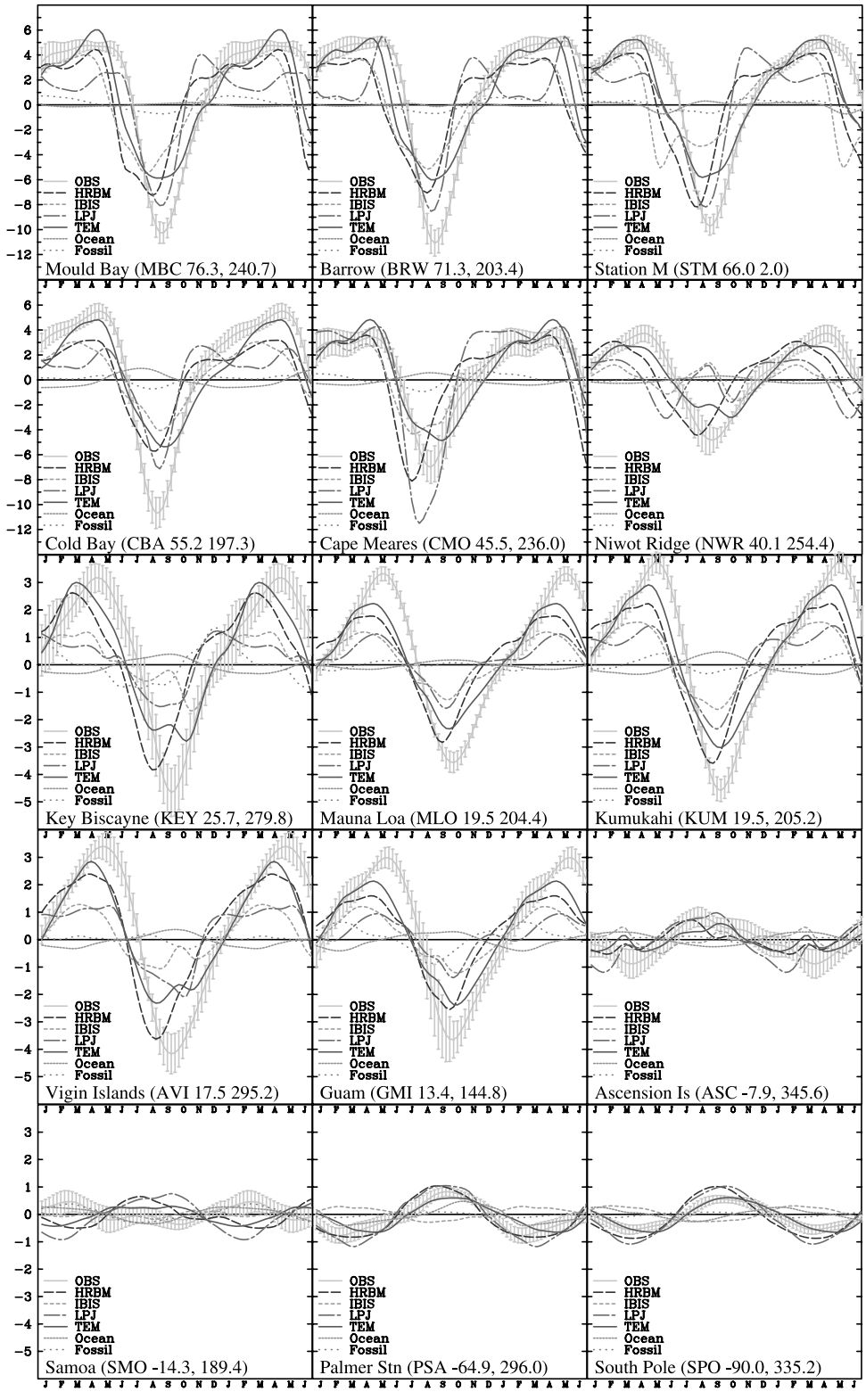

Figure 3. Average detrended seasonal cycle at 15 NOAA/CMDL monitoring sites for the *GLOBALVIEW-CO2* [1999] observations, and transport model runs with sources from HRBM, IBIS, LPJ and TEM. The pattern for each TCM result includes the contribution from the modeled fossil and ocean sources, which are also plotted. The individual captions detail the names and locations (latitude and longitude) of the stations and the three-letter abbreviations used in the text.

Table 1. RMS Differences for Seasonal Cycles[a]

Station	HRBM	IBIS	LPJ	TEM
spo	0.30	0.53	0.32	0.10
psa	0.22	0.65	0.26	0.20
smo	0.49	0.23	0.70	0.45
asc	0.31	0.50	0.42	0.29
Southern Hemisphere average	0.33	0.48	0.43	0.26
gmi	1.03	1.32	1.48	0.74
avi	1.22	1.72	1.52	0.90
kum	1.24	1.51	1.59	0.69
mlo	1.04	1.32	1.37	0.75
key	1.48	1.49	1.67	0.80
Tropical average	1.20	1.47	1.53	0.78
nwr	1.66	2.37	2.46	0.87
cmo	1.89	1.16	2.04	1.00
cba	2.37	2.61	2.73	1.87
stm	2.80	3.02	2.66	1.40
brw	3.00	2.65	2.83	1.75
mbc	2.78	2.59	2.47	1.69
Northern extratropics average	2.42	2.40	2.53	1.43
Global average	1.46	1.58	1.63	0.90

[a]Compare with Figure 3. Units are ppmv.

IBIS both have the maximum concentration early by several months, again indicating that these models are having phase problems in the northern midlatitudes.

[31] Table 2 gives the qualitative error estimates averaged for each station, and normalized against the station amplitude (such that the stations with small seasonal cycle amplitudes do not dominate the average). It is interesting to note that while LPJ produces small errors for the timing of the minimum concentrations, it does poorly for the maximum, again, perhaps due to the large outgassing in the autumn season in the high northern latitude.

4.3. Trends and Interannual Variability

4.3.1. Trends in Seasonal Cycle Amplitude

[32] In our transient TCM simulations we can examine the response of the terrestrial biosphere to the three scenarios modeled and the impacts on the simulated atmospheric seasonal cycle. We have calculated amplitude changes in the regionally aggregated TCM sources fields (Figure 5) and the seasonal amplitude trends in the observed and simulated atmospheric concentrations at our 15 NOAA/CMDL sites (Figure 6) for each scenario for each model. The analysis of the sources show that the runs with CO_2 fertilization alone have increasing seasonal cycle amplitude in most cases, although the magnitude varies considerably. The response to climate variability shows a decrease in the seasonal amplitude in most regions for most models with the exceptions of LPJ in the northern high latitudes and HRBM in the northern midlatitudes. The land-use change effect is small in the northern high latitudes, and tropics (again with the exception of HRBM in the northern tropics), but is the most important factor of all three scenarios in the northern midlatitudes giving rise to amplitude increases is all four models, although the increase in LPJ is small compared with the CO_2 effect.

[33] The trends in the sources in Figure 5 can be linked to the atmospheric seasonal cycle trends show in Figure 6, which shows the amplitude trends at each station for the observations (bold solid line with the uncertainty shown by

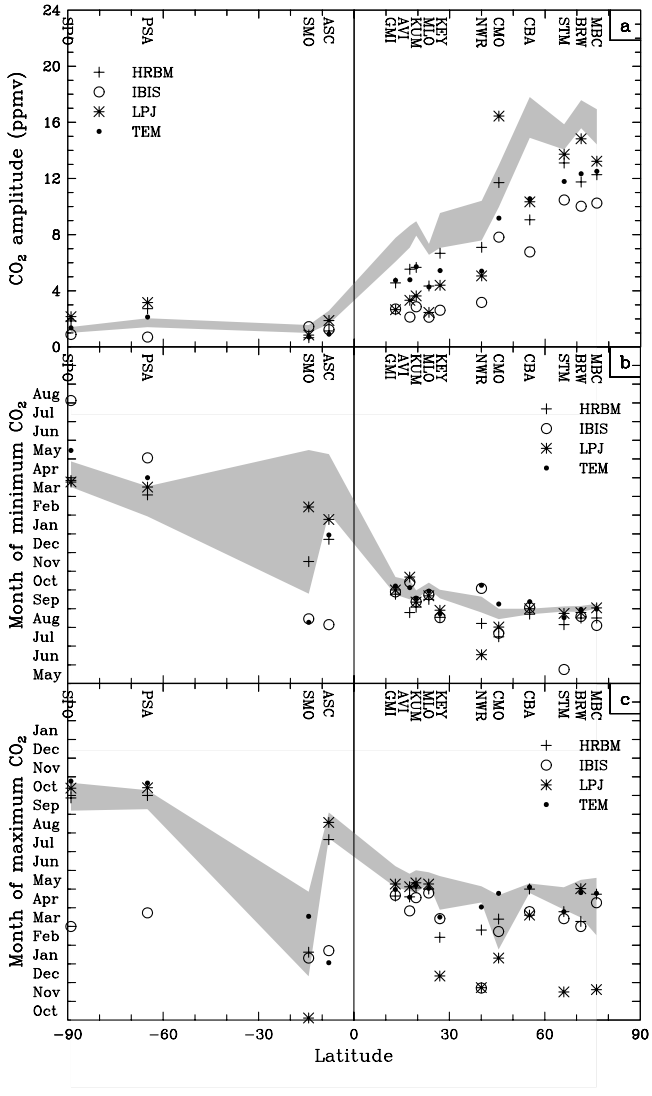

Figure 4. Seasonal cycle analysis at 15 NOAA/CMDL stations for the transport run using the S3 fluxes from the four TCMs. (a) Amplitude of the seasonal cycle, (b) timing of minimum concentrations, and (c) timing of the maximum concentrations. Note that the stations between 0° and 30°S have been equally spaced with latitude to make it easier to distinguish the different values. Each of the models is shown by a point symbol, while the observations are shown as a shaded area showing the range of 1 standard deviation about the mean.

Table 2. RMS Differences for Model Simulations Against Observations for Seasonal Cycles Amplitudes and Phasing of Minimum and Maximum Concentrations[a]

Feature	HRBM	IBIS	LPJ	TEM
Amplitude, ppmv	2.30	4.26	3.03	2.54
Minimum, months	0.83	1.18	0.59	0.53
Maximum, months	0.87	1.82	2.40	0.77

[a]Compare to Figure 4. Minimum and maximum timings are normalized against the amplitude of the seasonal cycle at each station.

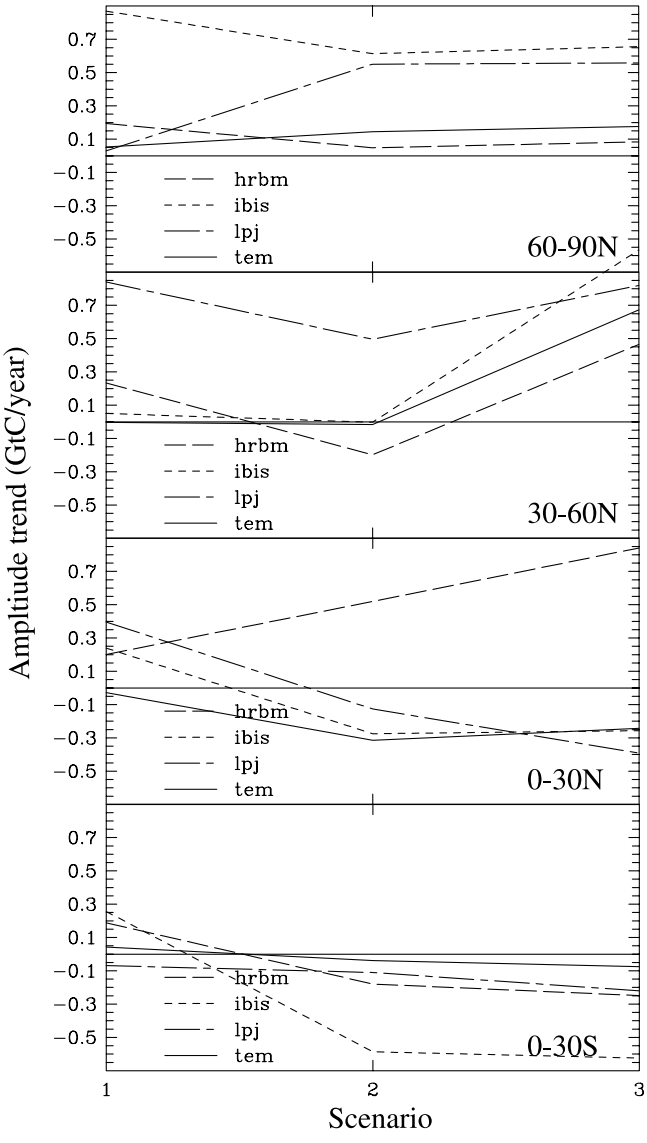

Figure 5. Changes in amplitude of the seasonal cycle of TCM sources aggregated over 30° latitude bands for each of the three scenarios: 1: increasing CO_2, 2: increasing CO_2 and climate variability, and 3: increasing CO_2, climate variability and land-use change.

the shading) and each model simulation. While over our short period the observed amplitude trends are subject to large uncertainties, the analysis has yielded results of interest. The observed trends in the southern hemisphere and tropics are generally small, the trend at NWR is negative (although with a lot of uncertainty) while in the high northern latitudes the observations yield the largest trends. Each of the simulations reproduce the main pattern of small trends in the Southern Hemisphere and larger positive trends in the northern high latitudes. HRBM and TEM show less variability in trend from station to station than IBIS and LPJ, and IBIS and LPJ simulate the negative trend at NWR. HRBM and TEM have the smaller amplitude trends in the sources in the northern middle and high latitudes, which is reflected in the atmospheric results, while IBIS's large trends in the source amplitude translate to large trends in the atmospheric simulation, in fact larger than the observation in the high latitudes. The S1 case for LPJ has a large anomalous trend at CMO, probably related to the large

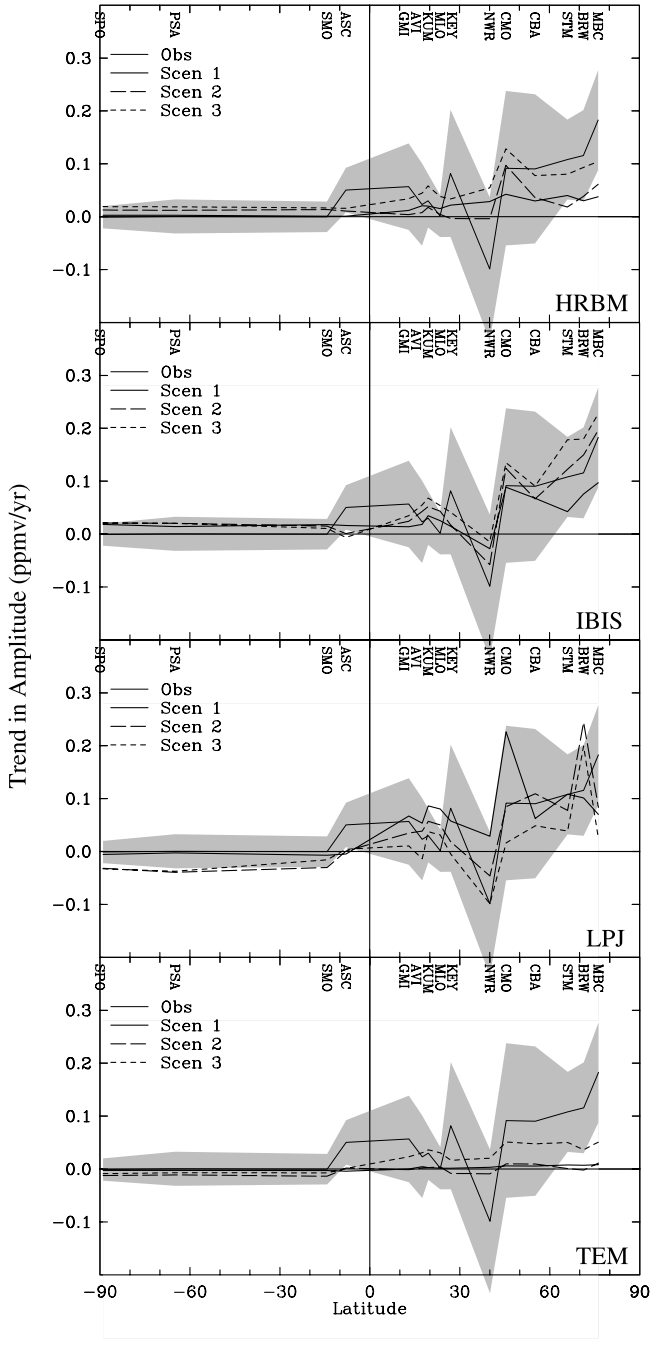

Figure 6. The trend in the seasonal cycle amplitude at the 15 NOAA/CMDL sites for each of the three TCM scenarios for (a) HRBM, (b) IBIS, (c) LPJ and (d) TEM. Trends were calculated by a linear regression through the time series of seasonal amplitudes. Shaded areas represent the observed gradient range as determined by the 90% confidence limits of the regression.

trend in response to increasing atmospheric concentration in S1 simulation.

4.3.2. Observed and Simulated Source and Concentration Anomalies

[34] Figure 7 shows the aggregated source anomalies over the 30° latitude bands, and the global anomalies. The variability in the 60–90°N band is relatively small, the 30–60°N region shows a trend with increasing carbon uptake by the vegetation, and the two tropical regions show El Ninõ/Southern Oscillation type variability which positive anomalies during El Ninõ periods (1983, 1987, and early 1990s). The global variability is dominated by the tropical signal. LPJ and IBIS tend to have more variability than TEM and HRBM. We can compare the global anomalies with the results from the inversion of *Bousquet et al.* [2000] which have similar patterns of uptake in El Ninõ years as seen in our TCM results, although the release in 1983 is greater in the TCMs, and the uptake in 1989 is also larger in the TCMs. The magnitude of variability in the results of *Bousquet et al.* [2000] is ±2 Gt C a^{-1} compared with the ±3 Gt C a^{-1} for LPJ and IBIS, ±2 Gt C a^{-1} for HRBM and ±1.5 Gt C a^{-1} for TEM. Comparisons of the S1, S2 and S3 simulations (not shown here) demonstrate that climate variability is the main driver for the variability in the fluxes.

[35] To investigate how the modeled source anomalies compare with the atmospheric CO_2 records we have calculated concentration anomalies for both the observations and simulated concentrations by again taking a 12-month running mean through the detrended time series. An example of the concentration anomalies is shown in Figure 8 which shows the 12-month running mean for the observations and LPJ simulations at Mauna Loa in the left panel, and the modeled anomalies plotted against the observed anomalies with a linear regression in the right panel. In this example the observations show large negative anomalies for 1983 and 1987, which may appear to disagree with the source anomalies in Figure 7, which have positive anomalies in these years. In fact, it should be expected that the concentration anomalies will lag the source anomalies as the concentration anomaly will continue to grow as long as the source anomaly is positive, such that the concentration anomaly will peak when the source anomaly returns to zero. On top of this, there will also be a lag between the source and concentrations due to the transport time.

[36] Figure 9 shows the slope and correlation coefficients for linear regressions between the observed and modeled anomalies for each model for each station. The models all have slopes of less than 0.4. The low values are largely due to the failure of the TCM-MATCH simulations to model the large negative anomalies in the El Ninõ years which exist at many of the observing sites. The reason for not modeling these excursions may be because they result from a decrease in the tropical ocean source during the early phase on El Ninõ when the coastal upwelling is suppressed, and we have not considered the interannual variability in the ocean fluxes in this study. In the Mauna Loa example in Figure 8 the model underestimates the 1983 and 1987 anomalies by around 0.4 ppmv, which is equivalent to a global source of about 1 Gt C, which is about the annual tropical release in our ocean simulation. If a significant portion of this release is suppressed in El Ninõ years this could explain our low regression slope values. Other possible explanations for the underestimates are presented in the discussion section.

[37] Table 3 shows the average regression slope and correlation for the 15 stations. HRBM and TEM show lower slopes and correlations than IBIS and LPJ, indicating that IBIS and LPJ have more interannual variability than HRBM and TEM. IBIS and LPJ also tend to have higher correlations. On average the correlation required for significance at the 90% confidence limit (as determined by the random phase test of *Ebisuzaki* [1997] is 0.43, which is satisfied at most stations by IBIS and LPJ, but very few by TEM and HRBM. The models show lower correlations at KEY, NWR and CMO. It could be that oceans or transport play a more important role at these sites, or that the land areas of the northern midlatitudes is the key region where the variability in the TCMs needs to be addressed.

5. Discussion

[38] This study has evaluated the seasonal cycle and interannual variability from simulations of process-based TCMs. These analyses indicate that the models differ in their abilities to simulate these aspects of the global carbon cycle. No model consistently performs better than the others, suggesting that all four require further development. Below, we discuss the results of these analyses, point out some of the limitations of the study, and identify further research required to improved our understanding of the role of terrestrial processes in the global carbon cycle.

5.1. Average Seasonal Cycle

[39] The comparison of the average atmospheric seasonal cycles for each of the TCM transport runs with the observations indicates that the models generally simulate the characteristics of the seasonal cycle, including the spatial trends in amplitude and phasing, although TEM and HRBM tend to perform better than LPJ and IBIS. These results, which were derived from the transient applications of the TCMs, are consistent with the results from other studies in which TCMs were run in equilibrium mode [see *Heimann et al.*, 1998; *Nemry et al.*, 1999; *McGuire et al.*, 2000]. The average seasonal cycle produced from the biosphere models for stations north of the tropics generally has too small a seasonal cycle, and the minimum concentration occurs too early in the year. *Heimann et al.* [1998] suggested that the biosphere models may overestimate the seasonal cycle of R_H. Reducing R_H during the growing season may allow NPP to dominate longer and thus correct the early phase and increase the seasonal amplitude. *McGuire et al.* [2000] demonstrated a possible mechanism to do this. By taking into account the thermal insulation effects of snow cover, this caused winter R_H to increase, while summer R_H decreased as the soil carbon pool was depleted. The overall effect was to increase the amplitude of the seasonal cycle of carbon uptake which led to an increase in the amplitude of the simulated atmospheric seasonal cycle of about 2 ppmv. As the TCMs tend to simulate the uptake of carbon too early in the spring, a better consideration of freeze-thaw dynamics by the models

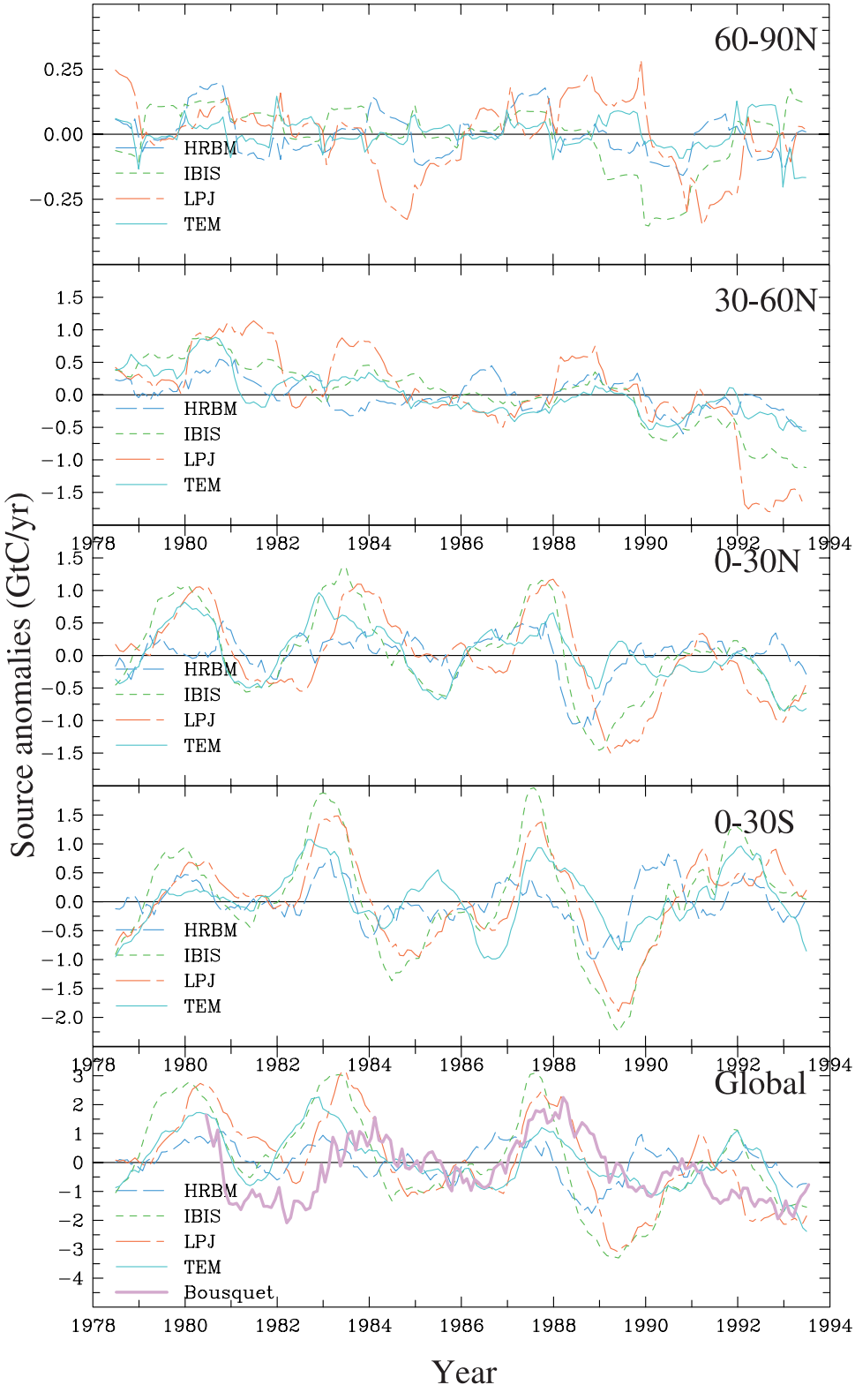

Figure 7. Source anomalies for each of the TCMs aggregated over 30° latitude bands, and the global sum. Anomalies were calculated by taking the 12-month running mean through the monthly source values. The bold solid line in the global panel is from the *Bousquet et al.* [2000] inversion.

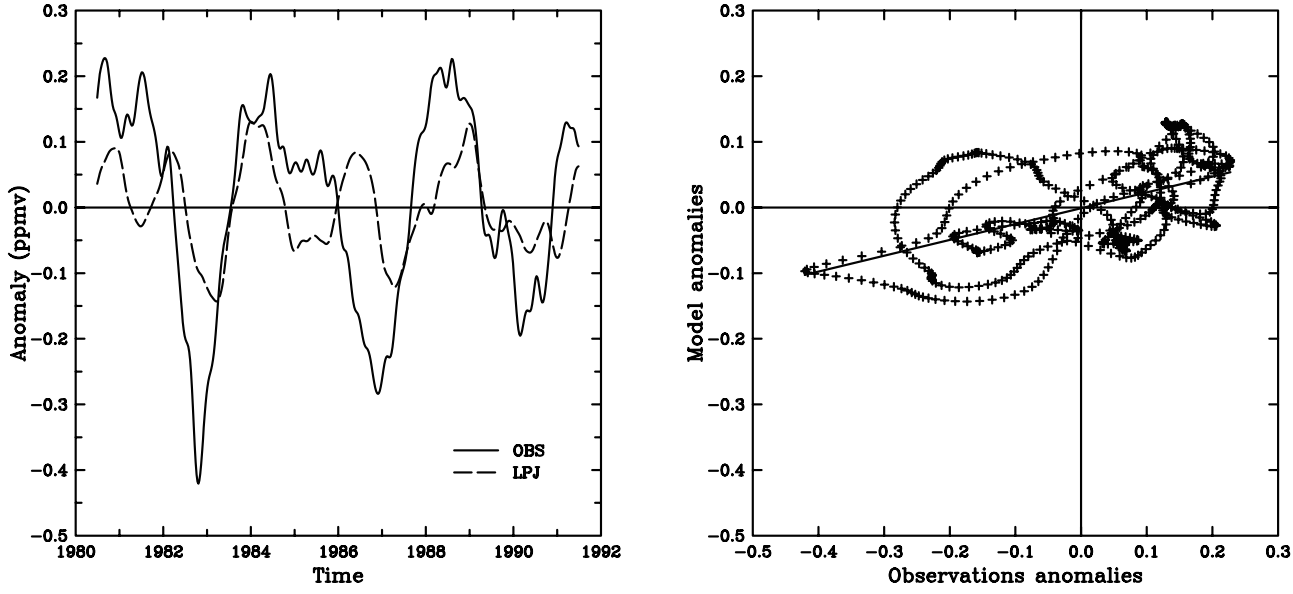

Figure 8. Example of the time series of the concentration anomalies and the regression. This example shows the comparison between the LPJ model and observations for Mauna Loa.

in high latitudes may improve the simulation of the average seasonal cycle at northern monitoring stations.

[40] One region of disagreement between observations and the model simulations is in the tropics at ASC and SMO where there is substantial interannual variability in the observations and little agreement among the models. Being close to the equator, these sites are sensitive to both the Northern and Southern Hemisphere fluxes and the vigorous vertical transport in the tropics due to the large amount of convective activity. Also, fire disturbance, which has not been considered in the seasonal cycle here, may play an important part in the seasonal cycle in this region [*Wittenberg et al.*, 1998; *Iacobellis et al.*, 1994]. The transport in the tropics has a large vertical component compared with

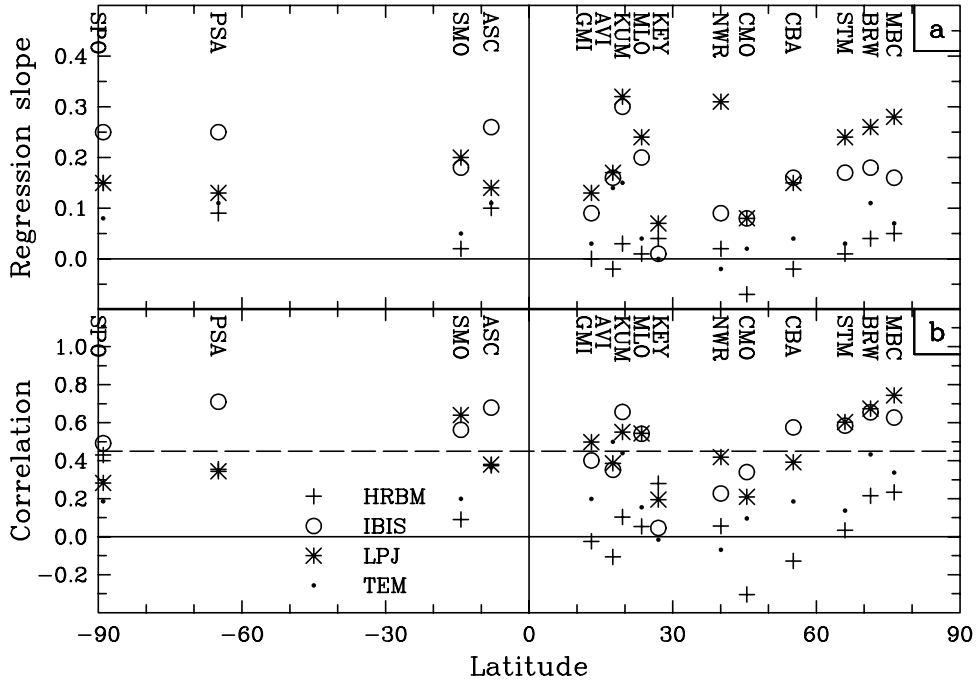

Figure 9. Results from regression analysis of simulated and observed concentration anomalies derived by taking the running mean through the trended time series. (a) Slope of the regression and (b) correlation of the simulated against observed anomalies. The dashed line shows the correlation requirement for 90% significance.

Table 3. Average Regression Slope and Correlation Values[a]

	HRBM	IBIS	LPJ	TEM
Regression	0.03	0.17	0.19	0.06
Correlation	0.11	0.50	0.46	0.23

[a]Compare to Figure 9.

other regions, as so much of the signal from the biosphere in this region is transported away from the surface and mixed with the upper troposphere. Thus, the impact of the region at the surface observing sites is relatively small. This is apparent when we consider that in the tropics the TCMs exhibit some of the strongest seasonality in the fluxes due to strong seasonality in rainfall [*Tian et al.*, 1998, 2000], but the simulated atmospheric CO_2 concentrations in the tropics show relatively small amplitudes in the seasonal cycle. This suggests that the combination of atmospheric measurements with a transport model is not the ideal way to evaluate the TCMs in the tropics. An alternative method for evaluating the TCMs in this region may be aircraft measurements of CO_2, or column integrals from satellite measurements [*Rayner and O'Brien*, 2001].

5.2. Trends and Interannual Variability

[41] The key advance in this study is the evaluation of the interannual variability from the TCMs. In general, the simulated trends in the amplitude of the seasonal cycle are within the uncertainties of the observed trends. There is large uncertainty in the observed trends because of the short period we examine The analysis of the TCM sources shows that CO_2 fertilization increased the amplitude, although the models vary in the magnitude, that climate variability acted to decrease the amplitude trend, and that land-use change in the northern midlatitudes is perhaps a significant factor in driving the amplitude increase. This is an important result, as the effect of land-use change in the midlatitudes is expected to decrease with time as the regrowth of the previously deforested areas is completed [*Pacala et al.*, 2000]. An important consideration here is that we have used constant fossil fuel fluxes, and that in reality the seasonality of the fossil fluxes is not zero. Therefore as the fossil fuel consumption increases, this amplitude will also increase. It is therefore important to do an additional experiment to investigate the impact of the fossil fuel increase on the amplitude trends.

[42] The global source anomalies compare well with the most recent estimates from atmospheric inversions [*Rayner et al.*, 1999; *Bousquet et al.*, 2000], both in magnitude and phase. In fact, LPJ and IBIS tend to show more variability than the inversions. The TCMs show that most of the global variability comes from the tropics, and that the interannual variability is driven almost entirely by the climate variability, but that that is expected as the CO_2 fertilization effect is fairly constant with time, and land-use change does not vary dramatically. The comparison of interannual variability between the observed and simulated concentration anomalies suggests that the models produce considerably less variability than the observations, but that a significant factor in the underestimation is that the negative concentration anomalies associated with El Ninõ are not well modeled, and that the ocean interannual variability could explain much of the discrepancy. It is also possible that the TCMs are not sensitive enough to interannual variability in the driving data (which is dominated by climate variability), or that the interannual variability in the transport is an important factor. Also, the transport model operates at a finite resolution and while the resolution used here (2.8° by 5.6°) is fair compared to other transport models, there is clearly the possibility that a portion of the atmospheric variability is numerically smoothed.

5.3. Limitations and Next Steps

[43] The flask sampling network we have used employs a selection criteria to reduce the influence of local sources which are difficult to model with our relatively course resolution. Also, the frequency of measurements is much less than the sampling in the transport model. These factors may lead to biases, the consideration of which are beyond the scope of this paper. It is important to keep in mind that this evaluation is also subject to uncertainty as the atmospheric data set is also influenced by small scale processes which are not represented in our transport model.

[44] The transport model also represents a source of uncertainty. The TransCom experiments have shown a range of transport behavior from different models. MATCH has been shown to be comparable with other widely used models, and its relatively fine resolution compared with GISS and TM2 models and sophisticated vertical parameterizations should allow for more accurate modeling of the transport. Evaluation and improvement of transport models is required for making progress in evaluating and improving TCMs. A potentially significant shortcoming of this study is that we have used model derived winds for our simulations. Clearly a useful experiment would be to repeat the transport runs using analyzed winds fields, such as the National Center for Environmental Prediction Global Reanalyses [*Kalnay et al.*, 1996].

[45] The observing network used in this study is mostly in the Western Hemisphere, and so the fluxes from the eastern hemisphere biosphere are not well represented in the atmospheric data. There are currently a few stations in Asia, with GLOBALVIEW sites in Korea, Mongolia and the South China Sea, but the sites have records starting in the early 1990s and are not appropriate for studying the 1980s. Once we are able to extend the simulations of the TCMs through the 1990s, the number of CO_2 observations available will increase substantially and we will be able to evaluate a much larger spatial domain. The longer time period will also allow a more rigorous investigation of the trends and interannual variability in the observed atmospheric seasonal cycle and the seasonal cycle simulated by the TCMs.

6. Conclusions

[46] The key findings in this study are that when fluxes from four TCMs are run through an atmospheric transport model, they are able to reproduce the main features of the atmospheric seasonal cycle. However, the TCMs tend to underestimate the amplitude of the seasonal cycle and have the phase around 1 month early in the Northern Hemi-

sphere. The main advance of this study has been to examine the contributions of the modeled terrestrial CO_2 flux interannual variability. A key process driving the increase in the amplitude of the midlatitude surface flux is land-use change, but the pattern is more difficult to decipher in the amplitude trends in the atmospheric simulation with different models showing different mechanisms for the amplitude increase. Overall, the global flux interannual variability agrees well with that predicted from an atmospheric inversion. However regionally, the modeled concentration anomalies are (shown to be driven by climate variability) reproduce less than half of the observed variability at the CO_2 observing stations, suggesting that either the ocean variability is a key factor, that models are not sensitive enough to the driving data, or that interannual variability in transport is also an important factor.

[47] While the models produce some similar results, there are also some differences. Two of the models (TEM and HRBM) tend to do better at modeling the characteristics of the average seasonal cycle (amplitude and phasing), while the other two models (LPJ and IBIS) are better at representing the interannual variability in the fluxes. The reasons for the differences are complex (processes modeled, i.e., fire disturbance in IBIS, or the inclusion of the nitrogen cycle in TEM, or that HRBM is a statistically based model, and also the different algorithms and parameterizations) and determining the causes for the differences is beyond the scope of this study. However the results highlights the need to choose a model that is appropriate to the task at hand.

[48] **Acknowledgments.** This work was conducted as part of the Carbon Cycle Model Linkage Project with support from the Electric Power Research Institute, from the Land Cover Land Use Change Program of the National Aeronautics and Space Administration, and from the National Science Foundation. This work was supported in part by a grant of HPC time from the Arctic Region Supercomputing Center. The authors would like to thank Philippe Bousquet et al. for the use of results from their 2000 *Science* paper, and Scott Doney (NCAR) and two anonymous reviewers for critical assessment of the manuscript.

References

Andres, R. J., G. Marland, I. Fung, and E. Matthews, A $1° \times 1°$ distribution of carbon dioxide emissions from fossil fuel consumption and cement manufacture, 1950–1990, *Global Biogeochem. Cycles*, *10*, 419–429, 1996.

Battle, M., M. L. Bender, P. P. Tans, J. W. C. White, J. T. Ellis, T. Conway, and R. J. Francey, Global carbon sinks and their variability inferred from atmospheric O_2 and $\delta^{13}C$, *Science*, *287*, 2467–2470, 2000.

Bolin, B., R. Sukumar, P. Ciais, W. P. Cramer, P. Jarvis, H. Kheshgi, C. Nobre, S. Semenov, and W. Steffen, Global perspective, in *IPCC Special Report on Land Use, Land-Use Change and Forestry*, edited by R. T. Watson et al., pp. 23–51, Cambridge Univ. Press, New York, 2000.

Bousquet, P., P. Ciais, P. Peylin, M. Ramonet, and P. Monfray, Inverse modeling of annual atmospheric CO_2 sources and sinks, 1, Method and control inversion, *J. Geophys. Res.*, *104*, 26,161–26,178, 1999.

Bousquet, P., P. Peylin, C. LeQuéré, P. Friedlingstein, and P. P. Tans, Regional changes in carbon dioxide fluxes over land and oceans since 1980, *Science*, *290*, 1342–1346, 2000.

Chapin, F. S., S. A. Zimov, G. R. Shaver, and S. E. Hobbie, CO_2 fluctuations at high latitudes, *Nature*, *383*, 585–586, 1996.

Ciais, P., et al., Partitioning of ocean and land uptake of CO_2 as inferred by $\delta^{13}C$ measurements from the NOAA Climate Monitoring and Diagnostics Laboratory Global Air Sampling Network, *J. Geophys. Res.*, *100*, 5051–5070, 1995.

Cramer, W., D. W. Kicklighter, A. Bondeau, B. Moore III, G. Churlina, B. Nemry, A. Ruimy, A. L. Schloss, and the participants of the Potsdom NPP Model Intercomparison, Comparing global models of terrestrial net primary productivity (NPP): Overview and key results, *Global Change Biol.*, *5*, 1–15, 1999.

Dargaville, R. J., S. Doney, L. Kergoat, I. Y. Fung, and D. S. Schimel, Covariance between inter-annual variability in CO_2 sources and atmospheric transport, in paper presented at Fall Meeting 2000, AGU, San Francisco, Calif., 2000.

Denning, A. S., I. Y. Fung, and D. A. Randall, Latitudinal gradient of atmospheric CO_2 due to seasonal exchange with land biota, *Nature*, *376*, 240–243, 1995.

Doney, S. C., K. Lindsay, and J. K. Moore, Global ocean carbon cycle modeling, in *Ocean Biogeochemistry: A JGOFS Synthesis*, edited by M. Fasham et al., Springer-Verlag, New York, in press, 2002.

Ebisuzaki, W., A method to estimate the statistical significance of a correlation when the data are serially correlated, *J. Clim.*, *10*, 2147–2153, 1997.

Enting, I. G., On the use of smoothing splines to filter CO_2 data, *J. Geophys. Res.*, *92*, 10,977–10,984, 1987.

Erickson, D. J., III, P. J. Rasch, P. P. Tans, P. Friedlingstein, P. Ciais, E. Maier-Reimer, K. Six, C. A. Fischer, and S. Walters, The seasonal cycle of atmospheric CO_2: A study based on the NCAR community climate model (CCM2), *J. Geophys. Res.*, *101*, 15,079–15,097, 1996.

Esser, G., J. Hoffstadt, F. Mack, and U. Wittenberg, High resolution biosphere model (hrbm)-Documentation model version 3.00.00, in *Mitteilungen aus dem Institut fur Pflanzenokolgie der Justus-Liebig-Universitat Giessen*, vol. 2, edited by G. Esser, p. 70, Inst. fur Pflanzenokolgie der Justus-Liebig-Universitat Giessen, Giessen, Germany, 1994.

Fan, S., M. Gloor, J. Mahlman, S. Pacala, J. Sarmiento, T. Takahashi, and P. Tans, A large terrestrial carbon sink in North America implied by atmospheric and oceanic CO_2 data and models, *Science*, *282*, 442–446, 1998.

Feely, R. A., R. Wanninkhof, T. Takahashi, and P. Tans, Influence of el Nino on the equatorial Pacific contribution to atmospheric CO_2 accumulation, *Nature*, *398*, 597–601, 1999.

Foley, J. A., I. C. Prentice, N. Ramankutty, S. Levis, D. Pollard, S. Sitch, and A. Haxeltine, An integrated biosphere model of land surface processes, terrestrial carbon balance, and vegetation dynamics, *Global Biogeochem. Cycles*, *10*, 603–628, 1996.

GLOBALVIEW-CO2, Cooperative atmospheric data integration project: Carbon dioxide [CD-ROM], NOAA/CMDL, Boulder, Colo., 1999, (Also available on Internet via anonymous FTP to ftp.cmdl.noaa.gov, Path: ccg/co2/GLOBALVIEW).

Hack, J. J., Parameterization of moist convection in the NCAR community climate model, CCM2, *J. Geophys. Res.*, *99*, 5551–5568, 1994.

Heimann, M., et al., Evaluation of terrestrial carbon cycle models through simulations of the seasonal cycle of atmospheric CO_2: First results of a model intercomparison study, *Global Biogeochem. Cycles*, *12*, 1–24, 1998.

Holtslag, A. A. M., and B. A. Boville, Local versus nonlocal boundary-layer diffusion in a global climate model, *J. Clim.*, *6*, 1825–1842, 1993.

Houghton, R. A., The annual net flux of carbon to the atmosphere from changes in land use 1850–1990, *Tellus, Ser. B*, *51*, 298–313, 1999.

Hulme, M. A., 1951–80 global land precipitation climatology for the evaluation of general circulation models, *Clim. Dyn.*, *7*, 57–72, 1992.

Iacobellis, S. F., R. Frouin, H. Razafimpanilo, R. C. J. Somerville, and S. C. Piper, North African savanna fires and atmospheric carbon dioxide, *J. Geophys. Res.*, *99*, 8321–8334, 1994.

Jones, P. D., Hemispheric surface air temperature variations: A reanalysis and an update to 1993, *J. Clim.*, *7*, 1794–1802, 1994.

Joos, F., R. Meyer, M. Bruno, and M. Leuenberger, The variability in the carbon sinks as reconstructed for the last 1000 years, *Geophys. Res. Lett.*, *26*, 1437–1440, 1999.

Kalnay, E., et al., The NMC/NCAR 40-year reanalysis project, *Bull. Am. Meteorol. Soc.*, *77*, 437–471, 1996.

Keeling, C. D., T. P. Whorf, M. Wahlen, and J. van der Plicht, Interannual extremes in the rate of rise of atmospheric carbon dioxide since 1980, *Nature*, *375*, 666–670, 1995.

Keeling, C. D., J. F. S. Chin, and T. P. Whorf, Increased activity of northern vegetation inferred from atmospheric CO_2 measurements, *Nature*, *382*, 146–149, 1996.

Kohlmaier, G. H., E. O. Sire, A. Janecek, C. D. Keeling, S. C. Piper, and R. Revelle, Modeling the seasonal contribution of a CO_2 fertilization effect of the terrestrial vegetation to the amplitude increase in atmospheric CO_2 at Mauna Loa Observatory, *Tellus, Ser. B*, *41*, 487–510, 1989.

Law, R. M., et al., Variations in modelled atmospheric transport of carbon dioxide and the consequences for CO_2 inversions, *Global Biogeochem. Cycles*, *10*, 783–796, 1996.

Lee, K., R. Wanninkhof, T. Takahashi, S. C. Doney, and R. A. Feely, Low interannual variability in recent oceanic uptake of atmospheric carbon dioxide, *Nature*, *396*, 155–159, 1998.

LeQuéré, C., J. C. Orr, P. Monfray, O. Aumont, and G. Madec, Interannual

variabiity of the oceanic sink of CO_2 from 1979 through 1997, *Global Biogeochem. Cycles*, *14*, 1247–1266, 2000.

Mahowald, N. M., P. J. Rasch, B. E. Eaton, S. Whittlestone, and R. G. Prinn, Transport of ^{222}Radon to the remote troposphere using the model of atmospheric transport and chemistry and assimilated winds from ECMWF and the National Center for Environmental prediction/NCAR, *J. Geophys. Res.*, *102*, 28,139–28,151, 1997.

Marland, G., T. A. Boden, and R. J. Andres, Global, regional, and national CO_2-emissions, in *Trends: A Compendium of Data on Global Change*, Carbon Dioxide Inf. Anal. Cent., Oak Ridge Natl. Lab., U.S. Dep. of Energy, Oak Ridge, Tenn., 2002.

Masarie, K. A., and P. P. Tans, Extension and integration of atmospheric carbon dioxide data into a globally consistent measurement record, *J. Geophys. Res.*, *100*, 11,593–11,610, 1995.

McGuire, A. D., J. M. Melillo, J. T. Randerson, W. J. Parton, M. Heimann, R. A. Meier, J. S. Clein, D. W. Kicklighter, and W. Sauf, Modeling the effect of snowpack on the heterotrophic respiration across northern temperate and high latitude regions: Comparison with measurements of atmospheric carbon dioxide in high latitudes, *Biogeochemistry*, *48*, 91–114, 2000.

McGuire, A., et al., Carbon balance of the terrestrial biosphere in the twentieth century: Analysis of COo_2, climate and land-use effects with four processed-based models, *Global Biogeochem. Cycles*, *15*, 183–203, 2001.

Melillo, J. M., et al., Vegetation/ecosystem modeling and analysis project: Comparing biogeography and biogeochemistry models in a continental-scale study of terrestrial ecosystem responses to climate change and double CO_2, *Global Biogeochem. Cycles*, *9*, 407–437, 1995.

Nemry, B., L. Francois, J. C. Gerard, A. Bondeau, M. Heimann, and PNMIG, Comparing global models of terrestrial net primary productivity (NPP): Analysis of the seasonal atmospheric CO_2 signal, *Global Change Biol.*, *5*, 65–76, 1999.

Pacala, S. W., et al., Carbon storage in the U.S. caused by land use change: Convergence of estimates from inventories of ecosystems and inversions of atmospheric data, paper presented at Fall Meeting 2000, AGU, San Francisco, Calif., 2000.

Ramankutty, N., and J. A. Foley, Characterizing patterns of global landuse: An analysis of global croplands data, *Global Biogeochem. Cycles*, *12*, 667–685, 1998.

Ramankutty, N., and J. A. Foley, Estimating historical changes in global land cover: Croplands from 1700 to 1992, *Global Biogeochem. Cycles*, *13*, 997–1027, 1999.

Randerson, J. T., M. V. Thompson, T. J. Conway, I. Y. Fung, and C. B. Field, The contribution of terrestrial sources and sinks to trends in the seasonal cycle of atmospheric carbon dioxide, *Global. Biogeochem. Cycles*, *11*, 535–560, 1997.

Randerson, J. T., C. B. Field, I. Y. Fung, and P. P. Tans, Increases in early season ecosystem uptake explain recent changes in the seasonal cycle of atmospheric CO_2 at high northern latitudes, *Geophys. Res. Lett.*, *26*, 2765–2768, 1999.

Rasch, P., N. M. Mahowald, and B. E. Eaton, Representations of transport, convection and the hydrologic cycle in chemical transport models: Implications for the modeling of short lived and soluble species, *J. Geophys. Res.*, *102*, 28,127–28,138, 1997.

Rayner, P. J., and D. M. O'Brien, The utility of remotely sensed CO_2 concentration data in surface inversions, *Geophys. Res. Lett.*, *28*, 175–178, 2001.

Rayner, P. J., I. G. Enting, R. J. Francey, and R. L. Langenfelds, Reconstructing the recent carbon cycle from atmospheric CO_2, $\delta^{13}C$ and O_2/N_2 observations, *Tellus, Ser. B*, *51*, 213–232, 1999.

Schimel, D., et al., Carbon storage by natural and agricultural ecosystems of the US 1980–1993, *Science*, *287*, 2004–2006, 2000.

Sitch, S., The role of vegetation dynamics in the control of atmospheric CO_2 content, Ph.D. thesis, Lund Univ., Lund, Sweden, 2000.

Tian, H., J. M. Melillo, D. W. Kicklighter, A. D. McGuire, J. V. K. Helfrich, B. Moore, and C. Vörösmarty, Effect of interannual climate variability on carbon storage in amazonian ecosystems, *Nature*, *396*, 664–667, 1998.

Tian, H., J. M. Melillo, D. W. Kicklighter, and A. D. McGuire, The sensitivity of terrestrial carbon storage to historical climate variability and atmospheric CO_2 on the United States, *Tellus, Ser. B*, *51*, 414–452, 1999.

Tian, H., J. M. Melillo, D. W. Kicklighter, A. D. Mcguire, J. Helfrich, B. Moore, and C. J. Vörösmarty, Climatic and biotic controls on annual carbon storage in Amazonian ecosystems, *Global Ecol. Biogeogr.*, *9*, 315–336, 2000.

Waugh, D. W., Three-dimensional simulations of long-lived tracers using winds from MACCM2, *J. Geophys. Res.*, *102*, 21,493–21,513, 1997.

Wittenberg, U., M. Heimann, G. Esser, A. D. McGuire, and W. Sauf, On the influence of biomass burning on the seasonal CO_2 signal as observed at monitoring stations, *Global Biogeochem. Cycles*, *12*, 531–544, 1998.

Zimov, S. A., S. P. Davidov, G. M. Zimova, A. I. Davidova, F. S. Chapin, M. C. Chapin, and J. F. Reyolds, Contribution of disturbance to increasing seasonal amplitude of atmospheric CO_2, *Science*, *284*, 1973–1976, 1999.

J. S. Clein and R. A. Meier, Institute of Arctic Biology, University of Alaska, P.O. Box 700, Fairbanks, AK 99775, USA. (fnjsc4@uaf.edu; fnram2@uaf.edu)

R. J. Dargaville, Laboratoire des Sciences du Climate et de l'Environnement CEA/CNRS, L'Orme des Merisiers, Bat 709 Gif-sur-Yvette F-91191, France. (dargavil@lsce.saclay.cea.fr)

G. Esser, T. Reichenau, and U. Wittenberg, Institut für Pflanzenökologie, Justus-Liebeg-Universität, IFZ, Heinrich-Buff-Ring 26-32, D-35392 Giessen, Germany. (gerd.esser@bot2.bio.uni-giessen.de; tim.reichenau@bio.uni-giessen.de; uwe.wittenberg@merck.de)

J. Foley and N. Ramankutty, Center for Sustainability and the Global Environment (SAGE), University of Wisconsin, 1710 University Avenue, Madison, WI 53726, USA. (jfoley@wisc.edu; ramanku@wisc.edu)

M. Heimann, J. Kaplan, and I. C. Prentice, Max-Plank Institut für Biogeochemie, Carl-Zeiss-Promenade 10, D-07745 Jena, Germany. (martin.heimann@bgc-jena.mpg.de; colin.prentice@bgc-jena.mpg.de; jkaplan@bgc-jena.mpg.de)

F. Joos, Physics Institute, University of Bern, Sidlerstrasse 5, CH-3012 Bern, Switzerland. (joos@climate.unibe.ch)

D. W. Kicklighter, J. M. Melillo, and H. Tian, Ecosystem Center, Marine Biological Laboratory, Woods Hole, MA 02543, USA. (dkick@mbl.edu; jmelillo@mbl.edu; htian@mbl.edu)

A. D. McGuire, U. S. Geological Survey, Alaska Cooperative Fish and Wildlife Research Unit, University of Alaska, Fairbanks, AK 99775, USA. (ffadm@uaf.edu)

B. Moore III and A. Schloss, Complex Systems Research Center, Institute for the Study of Earth, Oceans and Space, University of New Hampshire, 39 College Road, Durham, NH 03824, USA. (b.moore@unh.edu; annette.schloss@unh.edu)

S. Sitch, Potsdam Institut for Climate Impact Research, P.O. Box 60 12 03, D-14412 Potsdam, Germany. (sitch@pik-potsdam.de)

L. J. Williams, Electric Power Research Institute, 3412 Hillview Avenue, Palo Alto, CA 94304, USA. (ljwillia@epri.com)